

Article

Direct Base-Assisted C-H Cyclonickelation of 6-Phenyl-2,2'-bipyridine

Nicolas Vogt ¹, Vasily Sivchik ^{2,3,*}, Aaron Sandleben ¹, Gerald Hörner ^{4,5}
and Axel Klein ^{1,*}

¹ Department für Chemie, Institut für Anorganische Chemie, Universität zu Köln, Greinstraße 6, D-50939 Köln, Germany; nicolasvogt89@gmail.com (N.V.); aaronsandleben@googlemail.com (A.S.)

² Department of Chemistry, University of Eastern Finland, 80101 Joensuu, Finland

³ School of Chemistry, University of East Anglia, Earlham Road, Norwich NR4 7TJ, UK

⁴ Institut für Chemie, Anorganische Chemie IV, Universität Bayreuth, Universitätsstraße 30, D-95440 Bayreuth, Germany; gerald.hoerner@uni-bayreuth.de

⁵ Theoretische Chemie, Technische Universität Berlin, Straße des 17. Juni 135, D-10623 Berlin, Germany

* Correspondence: v.sivchik@uea.ac.uk (V.S.); axel.klein@uni-koeln.de (A.K.); Tel.: +49-221-470-4006 (A.K.)

Academic Editor: Burgert Blom

Received: 4 February 2020; Accepted: 20 February 2020; Published: 24 February 2020



Abstract: The organonickel complexes [Ni(Phbpy)X] (X = Br, OAc, CN) were obtained for the first time in a direct base-assisted arene C(sp²)-H cyclometalation reaction from the rather unreactive precursor materials NiX₂ and HPhbpy (6-phenyl-2,2'-bipyridine) or from the versatile precursor [Ni(HPhbpy)Br₂]₂. Different from previously necessary C-Br oxidative addition at Ni(0), an extended scan of reaction conditions allowed quantitative access to the title compound from Ni(II) on synthetically useful timescales through base-assisted C-H activation in nonpolar media at elevated temperature. Optimisation of the reaction conditions (various bases, solvents, methods) identified 1:2 mixtures of acetate and carbonate as unrivalled synergetic base pairs in the optimum protocol that holds promise as a readily usable and easily tuneable access to a wide range of direct nickelation products. While for the base-assisted C-H metalation of the noble metals Ru, Ir, Rh, or Pd, this acetate/carbonate method has been established for a few years, our study represents the leap into the world of the base metals of the 3d series.

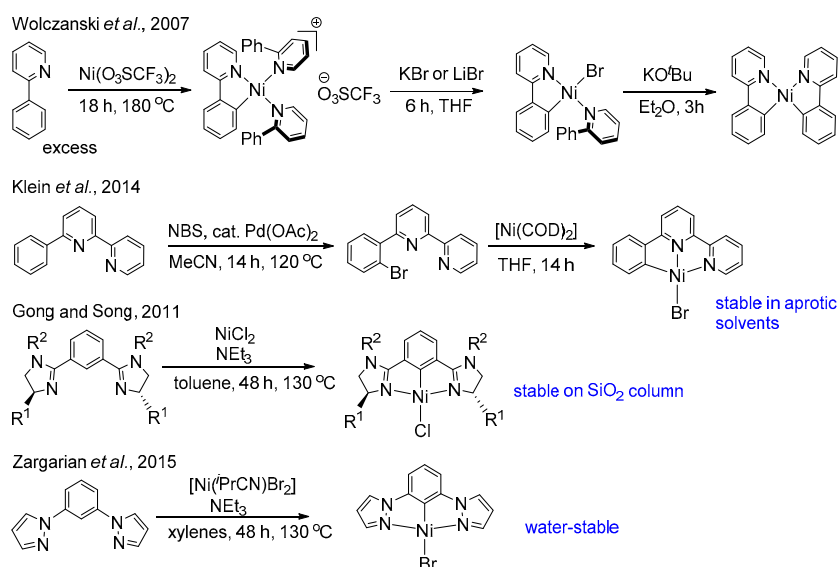
Keywords: cyclometalation; cyclonickelation; C-H activation; organonickel; base-assisted

1. Introduction

Metal-driven C(sp²)-H activation and turnover of the resulting metalated species in catalytic processes has for a long time been the domain of heavy elements from the 4d and 5d rows, such as ruthenium, iridium and, especially, palladium. Platinum-promoted C-H activation of hydrocarbons was one of the first milestones in this endeavour [1]. The intramolecular variant coined as cyclometalation initiated a period of rapid knowledge growth, owing to favourable metalation kinetics and thermodynamics [2,3]. Von Zelewsky et al. prepared the first biscycloplatinated derivatives of 2-phenylpyridine by transmetalation of the carbolithiated precursor back in the 1980s as well as discovered the intriguing luminescence of the obtained cyclometalated compounds [4]. Later, Constable et al. introduced cycloruthenation, cycloplatination, and cyclopalladation through C-H activation (direct cyclometalation) of aryl/N-donor moieties [5,6]. This straightforward synthetic approach coupled with the potential diversity of π -conjugated derivatives of C^N ligands to tailor photophysical properties led to intensive development in the field with more than 1000 congeners published today [7–19]. For Pd(II) salts (e.g., chloride or acetate) the direct cyclometalation of 2-phenylpyridine proceeds already at room temperature [6,14,20]. Not surprisingly, a considerable number of π -conjugated C^N-derivatives

are reported with interesting photophysical and biomedical properties [20,21]. Moreover, the ease of cyclopalladation resulted in the development of ground-breaking catalytic technologies based on Pd-catalysed directed C–H functionalisation [22–25].

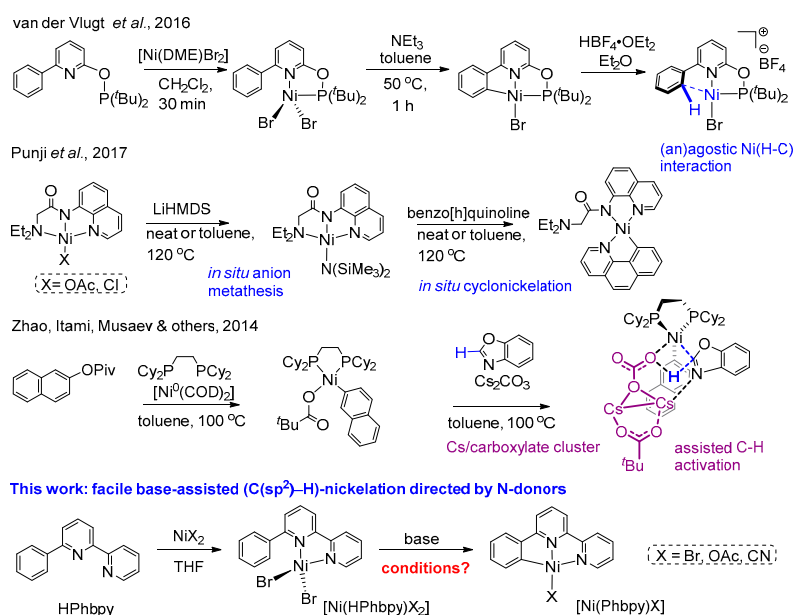
In sharp contrast to the literally thousands of examples available for Pd(II) and Pt(II), cyclometalated Ni(II) derivatives of nitrogen-donating π -conjugated moieties have remained rare species, although the first example of a cyclometalated Ni(II) complex, [Ni(Cp)(*o*-phenylazo)-phenyl], was prepared from [Ni(Cp)₂] (Cp[−] = cyclopentadienide) in 1963 [26]. Van Koten et al. introduced two approaches for the synthesis of Ni(N[^]C[^]N)-pincer complexes: (a) transmetalation of a Au(I) precursor; or (b) oxidative addition of zero-valent nickel to the bromoaryl precursor [27]. Much later, Wolczanski et al. directly metalated 2-phenylpyridine under harsh heating conditions (Scheme 1) [28], whereas Klein et al. performed a two-step cyclometalation via Pd-directed *ortho*-bromination of 6-phenyl-2,2'-bipyridine followed by the oxidative addition of zero-valent nickel, akin to van Koten's approach [29,30]. Direct, base-assisted metalation with NiCl₂ was demonstrated by Gong and Song in a pincer topology [31] and, in a similar approach by Zargarian et al. [32], it was found to be also feasible in macrocyclic N[^]C[^]N[^]C or N[^]C[^]N[^]N setups [33]. These reactions were considered to be electrophilic substitutions (H⁺ versus Ni(II)) that are archetypal for Pt(II) and Pd(II) complexes [1,25] but quite unique for Ni(II). Mechanistic insights were provided by van der Vlugt et al. for the formation of a [Ni(CNP)Br] pincer complex from the tetrahedral [Ni(HC[^]N[^]P)Br₂] precursor using NEt₃ as a base (Scheme 2) [34]. The isolation of a tri-coordinated T-shaped Ni complex with weak (an)agostic Ni \cdots (H-C) interaction invokes C-H bond coordination to Ni(II), forming a sigma-complex as a key step of the process with base neutralising the proton outside of the coordination sphere.



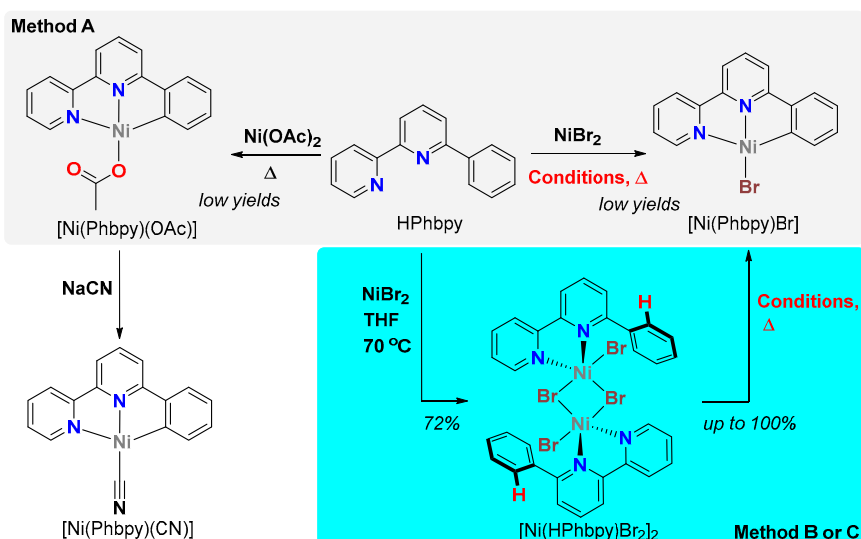
Scheme 1. Cyclonickelation of C(sp²)-H bonds with monodentate and bidentate N-heterocyclic directing groups.

Evidence for an inner-sphere attack of coordinated base was provided by Punji et al., who proposed the anion exchange of chloride or acetate by bis(trimethylsilyl)amide as a step precluding N-directed C-H bond activation under solvent-free conditions [35] (Scheme 2). In keeping with this, Musaev et al. suggested a cesium/carboxylate cluster as the active basic principle based on computational studies [36]. The latter treatment appears to be the most comprehensive one to explain the “carboxylate effect”, which is a recurrent motif in metalation at d⁸ metal centres, as reviewed a while ago by Ackermann [37] and recently discussed in deep mechanistic detail by Macgregor et al. for Ru, Ir, Rh, or Pd systems [38–40]. Schafer, Love et al. elegantly adopted this motif for the C-H activation of H₃C-N(Cy)C(O)N(H)(quinolin-8-yl), forming [Ni(-CH₂-N(Cy)(O)N(quinolinyl))(PEt₃)] [41].

Herein, we describe the development of a user-friendly protocol for a quantitative direct, base-assisted C(sp²)-H cyclonickelation procedure, relying on a simple *ortho*-phenyl pyridine system and NiBr₂ as the starting material. As a generic prototype of (di)nitrogen-directing moieties, we have selected 6-phenyl-2,2'-bipyridine (HPhbp), rendering the protocol suitable for a wide range of bidentate and tridentate ligands. Bidentate directional group assisted C-H activations have recently gained high interest in organometallic catalysis [36,37,42–45]. In a thorough and comprehensive scan of the reaction conditions (solvent; counter ion; temperature; external base(s); Schemes 2 and 3) we identified the combination of high-boiling nonpolar solvents and acetate/carbonate as a homogeneous/heterogeneous base couple to enable rather rapid and very efficient nickelation.



Scheme 2. Examples of base-assisted cyclonickelations and scope of this work.



Scheme 3. Cyclonickelation methods A–C and prepared compounds.

2. Results

We worked out different procedures for the direct C-H cyclonickelation of 6-phenyl-2,2'-bipyridine (HPhbp) to yield the previously reported red complex $[\text{Ni}(\text{Phbp})\text{Br}]$ (Scheme 3) [29,30].

The first synthesis attempts using NiBr₂ and HPhbpy in boiling ethanol or methanol were unsuccessful. After the initial dissolution of the precursor materials, the typical red colour was observed. However, further reaction and isolation yielded grey-green materials. This is in line with earlier reports on the title complex [29,30] and related work on the complex [Ni(Mes)(bpy)Br] (Mes = 2,4,6-trimethylphenyl; bpy = 2,2'-bipyridine), which decomposes in protic solvents yielding greenish octahedral Ni(II) species [46]. Avoiding protic solvents and working in vigorously dried solvents, we heated HPhbpy with NiBr₂ in toluene, but no yield was observed after 60 h at 130 °C (Table 1, entry 1). In keeping with the few literature reports, we ascribe the lack of reactivity to the lower basicity of the coordinated bromide ligand; similar observations have been reported by Campeau et al. [47] for a Pd catalysed bimolecular arylation and by Maseras and Echavarren et al. [48] for an intramolecular Pd-dependent arylation. In the following, we added external bases [49] such as NEt₃, NaHCO₃, Na₂CO₃, or Cs₂CO₃ to the reaction mixture (Entries 2–6). While for most reaction conditions the yields of [Ni(Phbpy)Br] were very poor (up to 2%), for Na₂CO₃/90 h/reflux, a crude yield of 19% was obtained (Table 1, Entry 6). In one of these experiments, MeOH was added to dissolve the starting materials, and the reaction time could be tremendously shortened (Entry 3). However, yield was poor due to decomposition, which was in line with the initial experiments. A further experiment in the melt (Entry 4) showed no yield.

Table 1. Essential parameters for the optimisation of the cyclonickelation of 6-phenyl-2,2'-bipyridine (HPhbpy).

	^a	NiX ₂	Base (eq.)	Solvent	Time (h)	T (°C)	Yield (%)	Analysis
1	A	NiBr ₂	no base	toluene	60	111 ^g	0	visual ^b
2	A	NiBr ₂	NEt ₃ (11.5)	toluene	48	111 ^g	1.5	¹ H NMR ^c
3	A	NiBr ₂	NaHCO ₃ (2)	toluene/MeOH	3	111 ^g	2.5	¹ H NMR
4	A	NiBr ₂	Na ₂ CO ₃ (4)	solid	1	170	0	visual ^b
5	B	NiBr ₂	Cs ₂ CO ₃ (2)	toluene	66	111 ^g	trace	¹ H NMR
6	B	NiBr ₂	Na ₂ CO ₃ (3)	toluene	90	111 ^g	19	¹ H NMR
7	C	[Ni(HPhbpy)Br ₂]	NaOtBu (2)	diethyl ether	16	23	0	¹ H NMR
8	C	[Ni(HPhbpy)Br ₂]	KOAc/K ₂ CO ₃ (2/4)	toluene	16	111 ^g	6	¹ H NMR
9	C	[Ni(HPhbpy)Br ₂]	KOAc/K ₂ CO ₃ (2/4)	toluene	62	111 ^g	28	¹ H NMR
10	A	Ni(OAc) ₂ ·4H ₂ O	-	toluene/EtOH//DME	15	111	5 ^d	XRD
11	A	Ni(OAc) ₂	-	solid	1	250	0 ^e	visual ^b
12	A	Ni(OAc) ₂	-	solid	1	180	4 ^f	XRD

^a Method A: Strictly direct cyclonickelation using NiBr₂ or Ni(OAc)₂. Method B: Cyclonickelation via in situ formation of [Ni(HPhbpy)Br₂]₂. Method C: Starting from isolated [Ni(HPhbpy)Br₂]₂. ^b The target complex has a characteristic red colour and can be easily traced visually in the reaction solution by the naked eye. ^c see Figures S1–S4 in the Supplementary Materials. ^d [Ni(Phbpy)(OAc)] was obtained. ^e Red material recrystallised from HOAc gave green-grey decomposed material. ^f Solid mixture heated while evaporated, trapped by NaCN in THF, and recrystallised from CH₂Cl₂, yielding [Ni(Phbpy)(CN)]. ^g The boiling temperature (reflux) is reported. Further details in Table S1 in the Supplementary Materials.

During this series of experiments, we noticed the quantitative formation of the non-cyclometalated 1:1 adduct [Ni(HPhbpy)Br₂]₂ upon heating NiBr₂ and HPhbpy in THF [50]. We were able to grow single crystals of this compound. Single-crystal XRD revealed a binuclear structure with an almost isotropic Ni₂(μ-Br)₂ diamond core with two triplet Ni(II) centres. Two other bromides are terminal ligands completing a five-coordinated trigonal bipyramidal geometry around nickel. (Figure 1; pertinent metrical data in Table S2 in the Supplementary Materials). In the following work, [Ni(HPhbpy)Br₂]₂ proved to be beneficial as a convenient, well-defined, and long-term storable form and was used as precursor (Table 1, Entries 7–9).

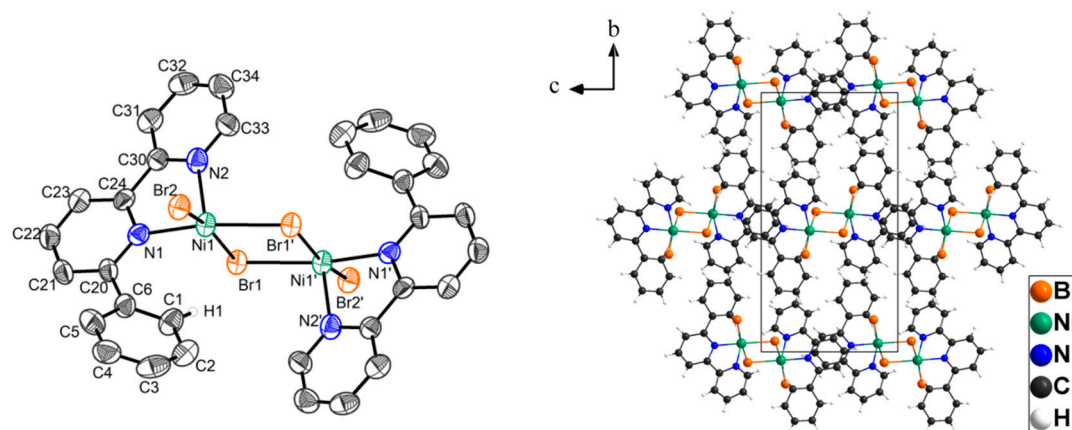


Figure 1. Ellipsoid view (two asymmetric units resulting in a binuclear structure) of $[\text{Ni}(\text{HPhbpy})\text{Br}_2]_2$ (left) and crystal structure of $[\text{Ni}(\text{HPhbpy})\text{Br}_2]_2$ viewed along the a axis (right). Ellipsoids are drawn at the 50% probability level.

Starting from $\text{Ni}(\text{OAc})_2 \cdot 4\text{H}_2\text{O}$, the acetato complex $[\text{Ni}(\text{Phbpy})(\text{OAc})]$ was obtained in traces (Entry 10), and the crystal and molecular structure could be solved (Figure 2, crystal and molecular data in Table S3 in the Supplementary Materials). The coordination geometry around $\text{Ni}(\text{II})$ is distorted square-planar.

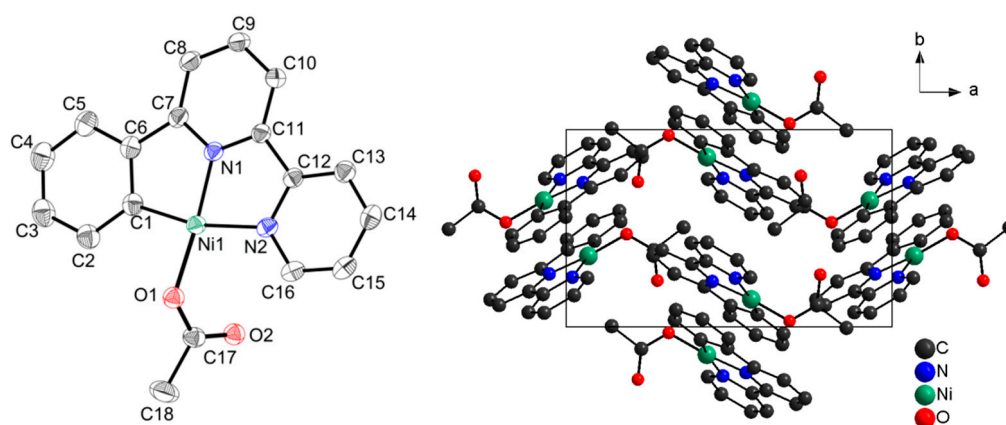


Figure 2. Ellipsoid view of $[\text{Ni}(\text{Phbpy})(\text{OAc})]$ (left) and crystal structure viewed along the c axis (right). Ellipsoids are drawn at the 50% probability level.

In a further experiment, anhydrous nickel acetate was used in a solid-state reaction to produce the acetato complex, but the product could not be isolated due to the degradation by acetic acid (Entry 11). Quenching the same reaction mixture with cyanide yielded some crystals of $[\text{Ni}(\text{Phbpy})(\text{CN})]$ (Entry 12, Figure S6, Table S4 and further details in the Supplementary Materials). Unfortunately, the crystal quality was too low for a satisfying crystal structure solution and refinement. However, the atom connectivity is unequivocal. Thus, in contrast to Br^- , acetate can obviously act as base.

Based on the encouraging 19% yield obtained from the reaction starting from the in situ formation of $[\text{Ni}(\text{HPhbpy})\text{Br}_2]_2$ (Table 1, Entry 6) we started a series of reactions using isolated $[\text{Ni}(\text{HPhbpy})\text{Br}_2]_2$. The reaction progress was monitored using UV-vis absorption spectroscopy with the spectrum of the previously reported $[\text{Ni}(\text{Phbpy})\text{Br}]$ [29] as reference. Using a 1:2 ratio and equimolar amounts (regarding the precursor) of KOAc and K_2CO_3 , we achieved a yield of 43% within three days of heating in toluene (Table 2). The yields further increased to 91% upon prolonged heating in chlorobenzene, reaching 98% in 1,2-dichlorobenzene and quantitative yield in p -xylene within 25 h (Figure 3). The use of the high-boiling benzonitrile did not yield the product. After 20 h, no yield

was observed and further heating at 200 °C for more than 60 h yielded a brown precipitated material that does not contain the targeted complex. We assume that the coordinating abilities of benzonitrile hamper the reaction by forming nitrile complexes [46], thus interfering with the formation of the intermediate $[\text{Ni}(\text{HPhbpy})\text{Br}_2]_2$. This is in line with low yields for Ni-catalysed $\text{C}(\text{sp}^2)\text{-H}$ and $\text{C}(\text{sp}^3)\text{-H}$ functionalisation of aminoquinoline in polar solvents such as DMSO, dioxane, and MeCN [51].

Table 2. Solvent influence on the optimised cyclonickelation reaction of HPhbpy ^a.

Entry	Solvent	Time (h)	T _{bat} (°C)	T _{b.p.} (°C)	E _T ^N ^b	Yield (%)
13	toluene	72	120	111	0.099	43
14	chlorobenzene	64	160	131	0.188	91
15	1,2-dichlorobenzene	25	190	180	0.225	98
16	<i>p</i> -xylene	25	160	138	0.074	100
17	benzonitrile	20	200	190	0.333	0
18	<i>p</i> -xylene ^c (from NiBr ₂)	64	160	138	0.074	93
19	1,2-dichlorobenzene ^d (no base)	64	190	180	0.225	15

^a Using $[\text{Ni}(\text{HPhbpy})\text{Br}_2]_2$ (65 mg, 0.14 mmol), KOAc (28 mg, 0.28 mmol), and K₂CO₃ (39 mg, 0.54 mmol), Dean–Stark apparatus, or activated molecular sieve. Yields as observed from UV-vis absorption measurements of the reaction solutions were based on the reported molar extinction coefficients of the long-wavelength maximum around 510 nm of the target complex $[\text{Ni}(\text{Phbpy})\text{Br}]$ [29,30]. ^b E_T^N = normalised empirical parameter of solvent polarity [52]. ^c Reaction starting from anhydrous NiBr₂. ^d Reaction without added base.

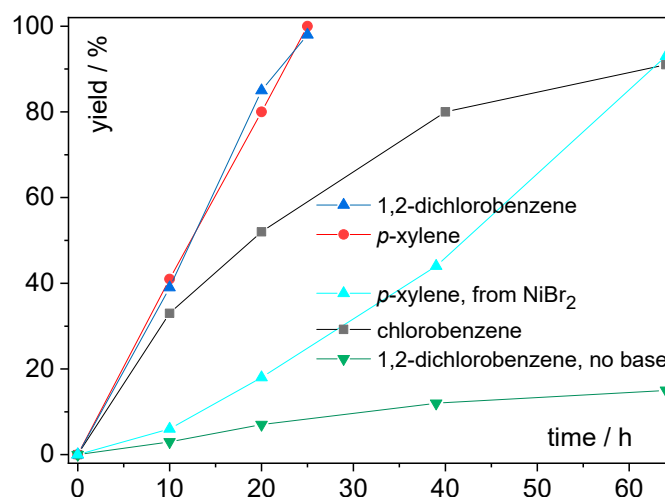


Figure 3. Yields of the cyclometalation reaction in various solvents, as monitored using UV-vis absorption spectroscopy. The traces represent the reaction entries 14, 15, 16, 18 and 19 in Table 2.

A detailed look on the time-dependence of the reaction for selected examples (Figure 3) shows that *p*-xylene and 1,2-dichlorobenzene reach high yields already after about 20 h, while chlorobenzene requires at least 40 h. Using NiBr₂ instead of $[\text{Ni}(\text{HPhbpy})\text{Br}_2]_2$ for the reaction in *p*-xylene under the same conditions afforded only 18% yield after 20 h but could be brought to 93% yield when heating for 64 h. This observation is in line with the assumed pre-formation of the *p*-xylene-soluble $[\text{Ni}(\text{HPhbpy})\text{Br}_2]_2$ from insoluble NiBr₂. Finally, a blank experiment in 1,2-dichlorobenzene (no external base) delivered a mediocre 15% yield after 64 h.

3. Discussion

Summarising the experimental results shows that (i) protic solvents and water-containing Ni salts must be avoided. Although they speed up reaction times due to perfect dissolution of the precursor compounds especially simple Ni(II) salts, the final product is quenched, presumably forming non-cyclometalated hexacoordinate Ni(II) species. (ii) The acetate/carbonate mixture is capable of driving the C-H metalation to completion, whereas single-component bases such as CO₃²⁻, HCO₃⁻,

t -OtBu, and NEt_3 promote the reaction on a trace level. (iii) The reaction proceeds preferably via the formation of the N \cdots N-coordinated intermediate $[\text{Ni}(\text{HPhbpy})\text{Br}_2]_2$. (iv) This precursor allows the use of high boiling nonpolar solvents, while protic solvents and water-containing polar solvents, which are necessary to dissolve the NiBr_2 precursor, can be avoided.

The observation of high reaction temperatures suggests a high activation barrier for the direct cyclonickelation of N-donor/aryl systems. Similarly, cyclonickelation to form C \cdots N or N \cdots C \cdots N chelates required harsh heating [28,31,32]. High reaction temperatures seem to be the price for starting from rather unreactive Ni(II) precursors and a not very reactive C(sp²)-H bond. In addition, the base-assisted N-H₂C(sp³)-H nickelation yielding $[\text{Ni}(-\text{CH}_2-\text{N}(\text{Cy})(\text{O})\text{N}(\text{quinolinyl})(\text{PEt}_3))]$ required temperatures above 70° [41]. In contrast to this, the C \cdots N \cdots P nickelation in the recently reported complex $[\text{Ni}(\text{HPh-Py-O-PR}_2)\text{Br}_2]$ (R = *t*Bu) proceeds at 50 °C in an hour [34]. The significantly lower activation barrier can be tentatively explained by the following factors: (i) the P-donor brings the Ni(II) centre closer to the C-H activation site to enable (an)agostic interactions, since phosphorus has a bigger covalent radius versus nitrogen (107 pm versus 71 pm), resulting in a Ni-P bond length of approximately 2.29 Å compared with the Ni-N bond of approximately 2.04 Å; (ii) this P-donor (decorated by two *t*Bu groups) is a much stronger σ -donor and perhaps a better π -acceptor than the N-site in our study. The Ni \cdots C distance in our precursor is 2.97(1) Å, which is quite short compared to the 3.039(3) Å of the phosphine complex. However, this distance is largely depending on the angle of the freely rotating phenyl group toward the binding plane, and the values represent only the solid state and not the molecules in solution. Moreover, the Ni-C bond in the cyclonickelated species $[\text{Ni}(\text{Ph-Py-O-PR}_2)\text{Br}]$ [34], $[\text{Ni}(\text{Phbpy})\text{Br}]$ [29], and $[\text{Ni}(\text{Phbpy})\text{OAc}]$ (Table S3) is of the same magnitude (approximately 1.9 Å). Therefore, the crystallographic data suggest that the difference in the electronic properties of the P- and N-donors rather than steric effects are responsible for the much lower activation barrier.

It is tempting to correlate the enhanced reaction efficiency with the high boiling points of these solvents, indicating simple Arrhenius behaviour. However, the complete lack of reactivity in benzonitrile as a solvent with a similarly high boiling point indicates that aspects of solvent polarity and coordination ability also affect the reaction progress. This generally agrees with the recent work of Sandford et al., who reported low cyclonickelation yields in polar-coordinating solvents [51]. In our study, alongside the series of solvents, an increase in polarity (E_T^N values) [52] leads to a decrease in activity. This inverse relationship points to a nonpolar transition state of the cyclometalation reaction, in stark contrast to the findings of Davies and Macgregor et al. [39], who inferred from substituent Hammett plots a substantial accumulation of positive charge in the transition state of a cycloruthenation reaction. Thus, in future work, we will model this reaction using density functional theory (DFT) methods.

4. Materials and Methods

4.1. Materials

Commercially available chemicals were purchased from Sigma-Aldrich, Acros, ABCR, or Fisher-Scientific and were used without further purification. Dry THF was obtained from distillation over sodium/potassium alloy. The preparation of *N*-(1-(2-pyridyl)-1-oxo-2-ethyl)pyridinium-iodide (Kroehnke salt) and 6-Phenyl-2,2'-bipyridine (HPhbpy) is described in the Supplementary Materials.

Preparation of $[\text{Ni}(\text{HPhbpy})\text{Br}_2]_2$ (adopted from Yang et al.) [50]: NiBr_2 (328 mg, 1.50 mmol), HPhbpy (348 mg, 1.50 mmol) in THF (125 mL) were heated under reflux for 15 h. After cooling to room temperature, a yellow solid was collected by filtration on a glass frit, washed using diethyl ether (3×10 mL), and dried in vacuo for 15 h. Yield: 72% (487 mg). Elemental analysis found (calc. for $\text{C}_{16}\text{H}_{12}\text{Br}_2\text{N}_2\text{Ni}$) C 42.62 (42.63); H 2.86 (2.68); N 6.23 (6.21)%.

4.2. Cyclonickelation Experiments

General considerations: In comparison with Pt or Pd congeners, cyclometalated Ni(II) complexes are less stable due to weaker Ni-C and Ni-N bonds [38,53]. The Ni-N bond, being also weaker than Ni-P bonds, is susceptible to facile ligand substitution by oxygen donors (e.g., alcohols) even in the case of chelating N^N-donors. [46]. The Ni-C bond is also chemically unstable. In addition to facile hydrolysis [46], oxygen insertion can occur in the presence of dioxygen with the formation of C-O-Ni bonds [54,55]. Thus, the cyclonickelation in this study was conducted under N₂ atmosphere in solvents purified by distillation over Na-benzophenone ketyl (toluene or THF) or rigorously dried molecular sieves (chlorobenzene, 1,2-dichlorobenzene, and benzonitrile).

Preparation of [Ni(Phbpy)Br] via C-H-activation: After a number of optimisation experiments (Tables 1 and 2), the reaction was carried out as follows. Under inert atmosphere [Ni(HPhbpy)Br₂]₂ (112.7 mg, 0.25 mmol, 1 eq.) was suspended in *p*-xylene (140 mL). After adding KOAc (25.5 mg, 0.25 mmol, 1 eq.) and K₂CO₃ (34.6 mg, 0.25 mmol, 1 eq.), the mixture was heated to reflux. For the separation of forming water, the reaction flask was interconnected by a glass frit filled with activated molecular sieve to the reflux condenser. After 25 h, the mixture was allowed to cool to room temperature, and the solvent was evaporated under reduced pressure. The deep red residue was dissolved in dry CH₂Cl₂ (100 mL) and filtered through a plug of Na₂SO₄/Celite. After evaporating the solvent, the product was received as a red powder. The yield was determined from the UV-vis absorption band of the product [Ni(Phbpy)Br] in THF (see Figure S5). The isolated material (183 mg, 0.495 mmol, 99%) was identified through its ¹H NMR spectrum [29,30].

From previous work, it was known that the [Ni(Phbpy)Br] is somewhat stable and soluble in CH₂Cl₂ (¹H NMR) and THF (reaction medium, crystallisation solvent). The complex has a characteristic red colour [29,30]. In the course of our investigation, we found that [Ni(Phbpy)Br] is insoluble in diethyl ether. Profiting from its moderate solubility and stability in acetone, ¹H and ¹H-¹H COSY NMR spectra was measured in acetone-d₆. Additionally, the compound can be recrystallised by the vapour diffusion of diethyl ether to CH₂Cl₂ or acetone at room temperature without special precautions. At the final stage, the red crystals can be quickly washed using methanol to eliminate the contaminant (yellow powder, presumably NiBr₂). Yet, [Ni(Phbpy)Br] degrades in methanol solution, as can be seen from the colour change from red to yellow and green, and ¹H NMR (CD₃OD) gave very broad signals indicating the formation of paramagnetic species. Details on the cyclometalation reactions yielding [Ni(Phbpy)X] (X = Br, OAc, CN) through base-assisted C-H activation (direct cyclometalation) are available in the Supplementary Materials.

Instrumentation: ¹H, ¹³C and ¹⁹F NMR spectra were recorded on a Bruker Avance II 300 MHz (¹H: 300 MHz, ¹³C: 75 MHz, ¹⁹F: 282 MHz, Ettlingen, Germany) equipped with a double resonance (BBFO) 5 mm observe probehead with z-gradient coil or on Bruker Avance 400 spectrometer (¹H: 400 MHz, ¹³C: 100 MHz, Ettlingen, Germany). Chemical shifts were relative to TMS. UV-vis absorption spectra were recorded on a Varian Cary 05E spectrophotometer (Troisdorf, Germany). Elemental analyses were obtained using a HEKAtech CHNS EuroEA 3000 analyzer (Wegberg, Germany). EI-MS spectra were measured using a Finnigan MAT 95 mass spectrometer (Bremen, Germany). Simulations were performed using ISOPRO 3.0 (Sunnyvale, CA, USA). Single crystal structure analysis (XRD): Measurement of [Ni(HPhbpy)Br₂]₂ was performed at 170(2) K using an IPDS IIT (STOE and Cie., Darmstadt, Germany) diffractometer, with Mo-K α radiation ($\lambda = 0.71073 \text{ \AA}$) employing ω - ϕ -2 θ scan technique. The structure was solved by direct methods using SIR 2014 [56], and refinement was carried out with SHELXL 2018 employing full-matrix least-squares methods on $F_0^2 \geq 2\sigma(F_0^2)$ [57]. The numerical absorption corrections (X-RED V1.22; Stoe & Cie, 2001, Darmstadt, Germany) were performed after optimising the crystal shapes using X-SHAPE V1.06 (Stoe & Cie, 1999, Darmstadt, Germany) [58]. The non-hydrogen atoms were refined with anisotropic displacement parameters without any constraints. The hydrogen atoms were included by using appropriate riding models. Measurement of [Ni(Phbpy)(OAc)] was conducted at 150 K. The X-ray diffraction data were collected with Bruker Kappa Apex-II (Ettlingen, Germany) diffractometer by using Mo-K α radiation

($\lambda = 0.71073 \text{ \AA}$). The APEX2 [59] program package was used for cell refinements and data reduction. Using OLEX2 [60], the structure was solved with the SHELXS program structure solution program using direct methods and refined with the SHELXL refinement package using least squares minimisation [61]. A numerical absorption correction (SADABS) [62] was applied to all data. The non-hydrogen atoms were refined with anisotropic displacement parameters without any constraints. All H atoms were positioned geometrically and constrained to ride on their parent atoms, with C–H = 0.95–0.99 Å and $U_{\text{iso}} = 1.2\text{--}1.5 U_{\text{eq}}$ (parent atom). Data of both structure solutions and refinements can be obtained free of charge at <https://summary.ccdc.cam.ac.uk/structure-summary-form> or from the Cambridge Crystallographic Data Centre, 12 Union Road, Cambridge, CB2 1EZ, UK (fax: +44-1223-336-033 or e-mail: deposit@ccdc.cam.ac.uk). CCDC 1956740 ([Ni(HPhbpy)Br₂]₂) and 1956739 ([Ni(Phbpy)(OAc)]).

5. Conclusions

Herein, we have addressed the central problem of a direct metalation of arene C(sp²)-H functions using rather unreactive Ni(II) precursors such as NiBr₂ or Ni(OAc)₂, which lifts the limitation of user-friendly metalation routines to the 4d and 5d rows. The target organonickel complex [Ni(Phbpy)Br] (HPhbpy = 6-phenyl-2,2'-bipyridine), which previously was accessible only from C-Br activation through a Ni(0) precursor, has now been obtained for the first time through C-H activation in a direct, base-assisted cyclonickelation. Optimal reaction conditions were identified to require (i) anhydrous precursor materials, (ii) elevated temperature, (iii) nonpolar media (*p*-xylene, (di)chlorobenzene), and (iv) the presence of carbonate and acetate as a synergetic base pair. On the other hand, the di-nitrogen coordination step of NiX₂ (X = Br, OAc) proceeds slowly in nonpolar media. Therefore, [Ni(HPhbpy)Br₂]₂ obtained by Ni(II) coordination in THF proved to be a convenient precursor for the direct, base-assisted metallation. The concerted fulfilment of all four criteria allows quantitative direct C-H activation on a synthetically reasonable timescale.

Although the reaction requires high temperatures > 100 °C, overall, the described quantitative direct nickelation appears superior to previous protocols with respect to a potential diversification. Variation of the substitution pattern of the metalated arene including deuteration and DFT modelling is subject of ongoing work. The high efficiency motivates a future extension to the more challenging cyclometalation of C(sp³)-H protoligands, which was elegantly demonstrated recently by Schafer, Love et al. for the formation of [Ni(-CH₂-N(Cy)C(O)N(quinoline-8-yl)(PEt₃))] [41]. While for the noble metals Ru, Ir, Rh, or Pd, the base-assisted C(sp²)-H deprotonation and metalation using acetate/carbonate has been established for a few years [38–40] our study represents an important step into the world of the base metals of the 3d series.

Supplementary Materials: Details on the C-H activation reactions and synthesis of the new complexes, NMR spectra, pictures of the crystal and molecular structure of [Ni(Phbpy)(CN)] and UV-vis absorption spectra with tables of important structural parameters of [Ni(HPhbpy)Br₂]₂, [Ni(Phbpy)(OAc)], and [Ni(Phbpy)(CN)] are available (see Supplementary Materials). The following are available online: Figure S1. 600 MHz ¹H NMR spectrum of [Ni(Phbpy)Br] in CD₂Cl₂. Figure S2. 400 MHz ¹H NMR spectrum of [Ni(Phbpy)Br] in CD₂Cl₂. Figure S3. 400 MHz ¹H NMR spectrum of [Ni(Phbpy)Br] in acetone-d₆. Figure S4. 400 MHz ¹H-¹H COSY spectrum of [Ni(Phbpy)Br] in acetone-d₆. Figure S5. UV-vis absorption spectra recorded during the reaction of [Ni(HPhbpy)Br₂]₂ in *p*-xylene in the presence of KOAc/K₂CO₃. Figure S6. Molecular structure of [Ni(Phbpy)(CN)] (left) and crystal structure viewed along the *c* axis (right). Note that the structure could not be solved satisfactorily. These plots show only preliminary results. Table S1. Parameters for the optimisation of the cyclonickelation of HPhbpy. Table S2. Crystal data, refinement parameters, and important bond parameters of the structure of the binuclear complex [Ni(HPhbpy)Br₂]₂. Table S3. Crystal data, structure refinement, and important bond parameters for [Ni(Phbpy)(OAc)]. Table S4. Crystal data for [Ni(Phbpy)(CN)].

Author Contributions: Conceptualisation, A.K. and V.S.; methodology, A.K. and G.H.; syntheses and analysis, V.S., N.V. and A.S.; crystal structures, A.S.; writing, review, and editing, V.S., A.K., and G.H.; visualisation, N.V.; funding acquisition, A.K. All authors have read and agreed to the published version of the manuscript.

Funding: The Deutsche Forschungsgemeinschaft DFG KL1194/15-1 is acknowledged for funding of this project.

Acknowledgments: G.H. thanks the DFG for financial support within the cluster of excellence UNICAT and SFB 840 (Von partikulären Nanosystemen zur Mesotechnologie) and Martin Kaupp (TU Berlin) for generous support.

We also grateful to Igor Koshevoy, Department of Chemistry, University of Eastern Finland, Joensuu for support and helpful discussions.

Conflicts of Interest: The authors declare no conflict of interest.

References

1. Labinger, J.A. Platinum-Catalyzed C–H Functionalization. *Chem. Rev.* **2017**, *117*, 8483–8496. [[CrossRef](#)] [[PubMed](#)]
2. Cope, A.C.; Siekman, R.W. Formation of Covalent Bonds from Platinum or Palladium to Carbon by Direct Substitution. *J. Am. Chem. Soc.* **1965**, *87*, 3272–3273. [[CrossRef](#)]
3. Cope, A.C.; Friedrich, E.C. Electrophilic Aromatic Substitution Reactions by Platinum(II) and Palladium(II) Chlorides on N,N-Dimethylbenzylamines. *J. Am. Chem. Soc.* **1968**, *90*, 909–913. [[CrossRef](#)]
4. Chassot, L.; Mueller, E.; Von Zelewsky, A. *cis*-Bis(2-phenylpyridine)platinum(II) (CBPPP): A Simple Molecular Platinum Compound. *Inorg. Chem.* **1984**, *23*, 4249–4253. [[CrossRef](#)]
5. Constable, E.C.; Henney, R.P.G.; Leese, T.A.; Tocher, D.A. Cyclometallation Reactions of 6-Phenyl-2,2'-bipyridine; a Potential C,N,N-Donor Analogue of 2,2':6',2''-Terpyridine. Crystal and Molecular Structure of Dichlorobis(6-phenyl-2,2'-bipyridine)ruthenium(II). *J. Chem. Soc., Dalton Trans.* **1990**, 443–449. [[CrossRef](#)]
6. Constable, E.C.; Henney, R.P.G.; Leese, T.A.; Tocher, D.A. Cyclopalladated and Cycloplatinated Complexes of 6-Phenyl-2,2'-bipyridine: Platinum-Platinum Interactions in the Solid State. *J. Chem. Soc. Chem. Commun.* **1990**, 513–515. [[CrossRef](#)]
7. Berenguer, J.R.; Lalinde, E.; Moreno, M.T. Luminescent cyclometalated-pentafluorophenyl Pt^{II}, Pt^{IV} and heteropolynuclear complexes. *Coord. Chem. Rev.* **2018**, *366*, 69–90. [[CrossRef](#)]
8. Tang, M.-C.; Chan, A.K.-W.; Chan, M.-Y.; Yam, V.W.-W. Platinum and Gold Complexes for OLEDs. *Top. Curr. Chem. (Z)* **2016**, *374*, 1–43. [[CrossRef](#)]
9. Kalinowski, J.; Fattori, V.; Cocchi, M.; Williams, J.A.G. Light-emitting devices based on organometallic platinum complexes as emitters. *Coord. Chem. Rev.* **2011**, *255*, 2401–2425. [[CrossRef](#)]
10. Williams, J.A.G. Metal complexes of pincer ligands: Excited states, photochemistry, and luminescence. *Top. Organomet. Chem.* **2011**, *40*, 89–130.
11. Yang, S.; Meng, F.; Wu, X.; Yin, Z.; Liu, X.; You, C.; Wang, Y.; Su, S.; Zhu, W. Dinuclear platinum(II) complex dominated by a zig-zag-type cyclometalated ligand: A new approach to realize high-efficiency near infrared emission. *J. Mater. Chem. C* **2018**, *6*, 5769–5777. [[CrossRef](#)]
12. Sivchik, V.; Sarker, R.K.; Liu, Z.-Y.; Chung, K.-Y.; Grachova, E.V.; Karttunen, A.J.; Chou, P.-T.; Koshevoy, I.O. Improvement of the Photophysical Performance of Platinum-Cyclometalated Complexes in Halogen-Bonded Adducts. *Chem. Eur. J.* **2018**, *24*, 11475–11484. [[CrossRef](#)]
13. Soellner, J.; Strassner, T. The “Enders Triazole” Revisited: Highly Efficient, Blue Platinum(II) Emitters. *Organometallics* **2018**, *37*, 1821–1824. [[CrossRef](#)]
14. Schulze, B.; Friebe, C.; Jäger, M.; Görls, H.; Birckner, E.; Winter, A.; Schubert, U.S. Pt^{II} Phosphors with Click-Derived 1,2,3-Triazole-Containing Tridentate Chelates. *Organometallics* **2018**, *37*, 145–155. [[CrossRef](#)]
15. Sesolis, H.; Chan, C.K.-M.; Gontard, G.; Fu, H.L.-K.; Yam, V.W.-W.; Amouri, H. Dinuclear (N[^]C[^]N) Pincer Pt(II) Complexes with Bridged Organometallic Linkers: Synthesis, Structures, Self-Aggregation, and Photophysical Properties. *Organometallics* **2017**, *36*, 4794–4801. [[CrossRef](#)]
16. Schneider, L.; Sivchik, V.; Chung, K.-Y.; Chen, Y.-T.; Karttunen, A.J.; Chou, P.-T.; Koshevoy, I.O. Cyclometalated Platinum(II) Cyanometallates: Luminescent Blocks for Coordination Self-Assembly. *Inorg. Chem.* **2017**, *56*, 4459–4467. [[CrossRef](#)] [[PubMed](#)]
17. Li, K.; Tong, G.S.M.; Wan, Q.; Cheng, G.; Tong, W.-Y.; Ang, W.-H.; Kwong, W.-L.; Che, C.-M. Highly phosphorescent platinum(II) emitters: Photophysics, materials and biological applications. *Chem. Sci.* **2016**, *7*, 1653–1673. [[CrossRef](#)]
18. Solomatina, A.I.; Chelushkin, P.S.; Abakumova, T.O.; Zhemkov, V.A.; Kim, M.; Bezprozvanny, I.; Gurzhiy, V.V.; Melnikov, A.S.; Anufrikov, Y.A.; Koshevoy, I.O.; et al. Reactions of Cyclometalated Platinum(II) [Pt(N[^]C)(PR₃)Cl] Complexes with Imidazole and Imidazole-Containing Biomolecules: Fine-Tuning of Reactivity and Photophysical Properties via Ligand Design. *Inorg. Chem.* **2019**, *58*, 204–217. [[CrossRef](#)]

19. Zhang, Y.; Luo, Q.; Zheng, W.; Wang, Z.; Lin, Y.; Zhang, E.; Lü, S.; Xiang, J.; Zhao, Y.; Wang, F. Luminescent cyclometallated platinum(II) complexes: Highly promising EGFR/DNA probes and dual-targeting anticancer agents. *Inorg. Chem. Front.* **2018**, *5*, 413–424. [[CrossRef](#)]
20. Chow, P.-K.; Cheng, G.; Tong, G.S.M.; Ma, C.; Kwok, W.-M.; Ang, W.-H.; Chung, C.Y.-S.; Yang, C.; Wang, F.; Che, C.-M. Highly luminescent palladium(II) complexes with sub-millisecond blue to green phosphorescent excited states. Photocatalysis and highly efficient PSF-OLEDs. *Chem. Sci.* **2016**, *7*, 6083–6098. [[CrossRef](#)]
21. Fleetham, T.; Li, G.; Li, J. Phosphorescent Pt(II) and Pd(II) Complexes for Efficient, High-Color-Quality, and Stable OLEDs. *Adv. Mater.* **2017**, *29*, 1601861. [[CrossRef](#)]
22. Hartwell, G.E.; Lawrence, R.V.; Smas, M.J. The Formation of Palladium(II)- and Platinum(II)-Carbon Bonds by Proton Abstraction from Benzo[h]quinoline and 8-Methylquinoline. *J. Chem. Soc., Chem. Commun.* **1970**, 912. [[CrossRef](#)]
23. Dick, A.R.; Hull, K.L.; Sanford, M.S. A Highly Selective Catalytic Method for the Oxidative Functionalization of C-H Bonds. *J. Am. Chem. Soc.* **2004**, *126*, 2300–2301. [[CrossRef](#)] [[PubMed](#)]
24. Thu, H.-Y.; Yu, W.-Y.; Che, C.-M. Intermolecular Amidation of Unactivated sp² and sp³ C-H Bonds via Palladium-Catalyzed Cascade C-H Activation/Nitrene Insertion. *J. Am. Chem. Soc.* **2006**, *128*, 9048–9049. [[CrossRef](#)] [[PubMed](#)]
25. Christman, W.E.; Morrow, T.J.; Arulsamy, N.; Hulley, E.B. Absolute Estimates of Pd^{II}(η²-Arene) C–H Acidity. *Organometallics* **2018**, *37*, 2706–2715. [[CrossRef](#)]
26. Kleiman, J.P.; Dubeck, M. The preparation of cyclopentadienyl [o-(phenylazo)phenyl]nickel. *J. Am. Chem. Soc.* **1963**, *85*, 1544–1545. [[CrossRef](#)]
27. Grove, D.M.; van Koten, G.; Ubbels, H.J.C.; Zoet, R. Organonickel(II) Complexes of the Terdentate Monoanionic Ligand o,o′-Bis[(dimethylamino)methyl]phenyl (N-C-N). Syntheses and the X-ray Crystal Structure of the Stable Nickel(II) Formate [Ni(N-C-N)O₂CH]. *Organometallics* **1984**, *3*, 1003–1009. [[CrossRef](#)]
28. Volpe, E.C.; Chadeayne, A.R.; Wolczanski, P.T.; Lobkovsky, E.B. Heterolytic CH-bond activation in the synthesis of Ni{(2-aryl-κC²)pyridine-κN}₂ and derivatives. *J. Organomet. Chem.* **2007**, *692*, 4774–4783. [[CrossRef](#)]
29. Klein, A.; Rausch, B.; Kaiser, A.; Vogt, N.; Krest, A. The cyclometalated nickel complex [(Phbpy)NiBr] (Phbpy[−] = 2,2′-bipyridine-6-phen-2-yl)—Synthesis, spectroscopic and electrochemical studies. *J. Organomet. Chem.* **2014**, *774*, 86–93. [[CrossRef](#)]
30. Sandleben, A.; Vogt, N.; Hörner, G.; Klein, A. On the Redox Series of Cyclometalated Nickel Complexes [Ni((R)Ph(R′)bpy)Br]^{+0/−2−} (H-(R)Ph(R′)bpy = substituted 6-phenyl-2,2′-bipyridine). *Organometallics* **2018**, *37*, 3332–3341. [[CrossRef](#)]
31. Shao, D.-D.; Niu, J.-L.; Hao, X.-Q.; Gong, J.-F.; Song, M.-P. Neutral and cationic chiral NCN pincer nickel(II) complexes with 1,3-bis(2′-imidazolyl)benzenes: Synthesis and characterization. *Dalton Trans.* **2011**, *40*, 9012–9019. [[CrossRef](#)] [[PubMed](#)]
32. Cloutier, J.P.; Vabre, B.; Mougang-Soumé, B.; Zargarian, D. Synthesis and Reactivities of New NCN-Type Pincer Complexes of Nickel. *Organometallics* **2015**, *34*, 133–145. [[CrossRef](#)]
33. Yang, C.; Wu, W.-D.; Zhao, L.; Wang, M.-X. Macrocyclic Aryl–Nickel(II) Complexes: Synthesis, Structure, and Reactivity Studies. *Organometallics* **2015**, *34*, 5167–5174. [[CrossRef](#)]
34. Jongbloed, L.S.; García-López, D.; van Heck, R.; Siegler, M.A.; Carbó, J.J.; van der Vlugt, J.I. Arene C(sp²)-H Metalation at Ni^{II} Modeled with a Reactive PONCPh Ligand. *Inorg. Chem.* **2016**, *55*, 8041–8047. [[CrossRef](#)] [[PubMed](#)]
35. Jagtap, R.A.; Soni, V.; Punji, B. Expedient and Solvent-Free Nickel-Catalyzed C–H Arylation of Arenes and Indoles. *ChemSusChem* **2017**, *10*, 2242–2248. [[CrossRef](#)] [[PubMed](#)]
36. Xu, H.; Muto, K.; Yamaguchi, J.; Zhao, C.; Itami, K.; Musaev, D.G. Key Mechanistic Features of Ni-Catalyzed C–H/C–O Biaryl Coupling of Azoles and Naphthalen-2-yl Pivalates. *J. Am. Chem. Soc.* **2014**, *136*, 14834–14844. [[CrossRef](#)]
37. Ackermann, L. Carboxylate-Assisted Transition-Metal-Catalyzed C–H Bond Functionalizations: Mechanism and Scope. *Chem. Rev.* **2011**, *111*, 1315–1345. [[CrossRef](#)]
38. Davies, D.L.; Macgregor, S.A.; McMullin, C.L. Computational Studies of Carboxylate-Assisted C-H Activation and Functionalization at Group 8-10 Transition Metal Centres. *Chem. Rev.* **2017**, *117*, 8649–8709. [[CrossRef](#)]

39. Alharis, R.A.; McMullin, C.L.; Davies, D.L.; Singh, K.; Macgregor, S.A. Understanding Electronic Effects on Carboxylate-Assisted C–H Activation at Ruthenium: The Importance of Kinetic and Thermodynamic Control. *Faraday Discuss.* **2019**, *220*, 386–403. [[CrossRef](#)]
40. Alharis, R.A.; McMullin, C.L.; Davies, D.L.; Singh, K.; Macgregor, S.A. The Importance of Kinetic and Thermodynamic Control when Assessing Mechanisms of Carboxylate-Assisted C–H Activation. *J. Am. Chem. Soc.* **2019**, *141*, 8896–8906. [[CrossRef](#)]
41. Beattie, D.D.; Grunwald, A.C.; Perse, T.; Schafer, L.L.; Love, J.A. Understanding Ni(II)-Mediated C(sp³)-H Activation: Tertiary Ureas as Model Substrates. *J. Am. Chem. Soc.* **2018**, *140*, 12602–12610. [[CrossRef](#)]
42. Rej, S.; Ano, Y.; Chatani, N. Bidentate Directing Groups: An Efficient Tool in C–H Bond Functionalization Chemistry for the Expedient Construction of C–C Bonds. *Chem. Rev.* **2020**. [[CrossRef](#)] [[PubMed](#)]
43. Sambiagio, C.; Schönbauer, D.; Blicke, R.; Dao-Huy, T.; Pototschnig, G.; Schaaf, P.; Wiesinger, T.; Zia, M.F.; Wencel-Delord, J.; Besset, T.; et al. A comprehensive overview of directing groups applied in metal-catalysed C–H functionalisation chemistry. *Chem. Soc. Rev.* **2018**, *47*, 6603–6743. [[CrossRef](#)] [[PubMed](#)]
44. Kommagalla, Y.; Chatani, N. Cobalt(II)-catalyzed CH functionalization using an N,N'-bidentate directing group. *Coord. Chem. Rev.* **2017**, *350*, 117–135. [[CrossRef](#)]
45. Tang, H.; Zhou, B.; Huang, X.-R.; Wang, C.; Yao, J.; Chen, H. Origins of Selective C(sp²)-H Activation Using Transition Metal Complexes with N,N-Bidentate Directing Groups: A Combined Theoretical–Experimental Study. *ACS Catal.* **2014**, *4*, 649–656. [[CrossRef](#)]
46. Feth, M.P.; Klein, A.; Bertagnolli, H. Investigation of the ligand exchange behaviour of square planar nickel(II) complexes by X-ray absorption spectroscopy and X-ray diffraction. *Eur. J. Inorg. Chem.* **2003**, 839–852. [[CrossRef](#)]
47. Sun, H.-Y.; Gorelsky, S.E.; Stuart, D.R.; Campeau, L.-C.; Fagnou, K. Mechanistic Analysis of Azine N-Oxide Direct Arylation: Evidence for a Critical Role of Acetate in the Pd(OAc)₂ Precatalyst. *J. Org. Chem.* **2010**, *75*, 8180–8189. [[CrossRef](#)]
48. Garica-Cuadrado, D.; de Mendoza, P.; Braga, A.A.C.; Maseras, F.; Echavarren, A.M. Proton-Abstraction Mechanism in the Palladium-Catalyzed Intramolecular Arylation: Substituent Effects. *J. Am. Chem. Soc.* **2007**, *129*, 6880–6886. [[CrossRef](#)]
49. Raamata, E.; Kaupmeesa, K.; Ovsjannikova, G.; Trummalb, A.; Kütta, A.; Saamea, J.; Koppela, I.; Kaljuranda, I.; Lippinga, L.; Rodimaa, T.; et al. Acidities of strong neutral Brønsted acids in different media. *J. Phys. Org. Chem.* **2013**, *26*, 162–170. [[CrossRef](#)]
50. Yang, P.; Yang, Y.; Zhang, C.; Yang, X.J.; Hu, H.M.; Gao, Y.; Wu, B. Synthesis, structure, and catalytic ethylene oligomerization of nickel(II) and cobalt(II) complexes with symmetrical and unsymmetrical 2,9-diaryl-1,10-phenanthroline ligands. *Inorg. Chim. Acta* **2009**, *362*, 89–96. [[CrossRef](#)]
51. Roy, P.; Bour, J.R.; Kampf, J.W.; Sanford, M.S. Catalytically Relevant Intermediates in the Ni-Catalyzed C(sp²)-H and C(sp³)-H Functionalization of Aminoquinoline Substrates. *J. Am. Chem. Soc.* **2019**, *141*, 17382–17387. [[CrossRef](#)]
52. Reichardt, C.; Welton, T. *Solvents and Solvent Effects in Organic Chemistry*, 4th ed.; WILEY-VCH Verlag GmbH & Co. KGaA: Weinheim, Germany, 2011; p. 455.
53. Hartwig, J.F. *Organotransition Metal Chemistry: From Bonding to Catalysis*; University Science Books: Millvalley, CA, USA, 2010; p. 9.
54. Pattanayak, P.; Pratihar, J.L.; Patra, D.; Burrows, A.; Mohan, M.; Chattopadhyay, S.; Lal Pratihar, J.; Patra, D.; Burrows, A.; Mohan, M.; et al. Regiospecific ortho-aromatic hydroxylation via cyclonickelation using hydrogen peroxide and other oxygen donors: Synthesis of metalloazosalophens. *Eur. J. Inorg. Chem.* **2007**, *2007*, 4263–4271. [[CrossRef](#)]
55. Sripothongnak, S.; Barone, N.; Ziegler, C.J. C–H bond activation and ring oxidation in nickel carbahemiporphyrazines. *Chem. Commun.* **2009**, *30*, 4584–4586. [[CrossRef](#)] [[PubMed](#)]
56. Burla, M.C.; Caliendo, R.; Carrozzini, B.; Cascarano, G.L.; Cuocci, C.; Giacobozzo, C.; Mallamo, M.; Mazzone, A.; Polidori, G. Crystal structure determination and refinement via SIR2014. *J. Appl. Crystallogr.* **2015**, *48*, 306–309. [[CrossRef](#)]
57. Sheldrick, G.M. SHELXL 2016. *Acta Crystallogr., Sect. A: Found. Crystallogr.* **2008**, *64*, 112–122.
58. X-RED32 1.31 & X-SHAPE; Version 1.06; STOE & Cie GmbH: Darmstadt, Germany, 2006.
59. APEX2—Software Suite for Crystallographic Programs; Bruker AXS, Inc.: Madison, WI, USA, 2010.

60. Dolomanov, O.V.; Bourhis, L.J.; Gildea, R.J.; Howard, J.A.K.; Puschmann, H. OLEX2: A Complete Structure Solution, Refinement and Analysis Program. *J. Appl. Crystallogr.* **2009**, *42*, 339–341. [[CrossRef](#)]
61. Sheldrick, G.M. Crystal Structure Refinement with SHELXL. *Acta Crystallogr. Sect. C: Struct. Chem.* **2015**, *71*, 3–8. [[CrossRef](#)]
62. Sheldrick, G.M. *SADABS-2008/1—Bruker AXS Area Detector Scaling and Absorption Correction*; Bruker AXS, Inc.: Madison, WI, USA, 2008.

Sample Availability: Samples of the compounds [Ni(Phbpy)Br], [Ni(HPhbpy)Br₂]₂, and [Ni(Phbpy)(OAc)] are available from the authors.



© 2020 by the authors. Licensee MDPI, Basel, Switzerland. This article is an open access article distributed under the terms and conditions of the Creative Commons Attribution (CC BY) license (<http://creativecommons.org/licenses/by/4.0/>).